UNIVERSITY *of York*

This is a repository copy of *Mass selection in laser-plasma ion accelerator on nanostructured surfaces*.

White Rose Research Online URL for this paper:
https://eprints.whiterose.ac.uk/id/eprint/113600/

White Rose
university consortium
Universities of Leeds, Sheffield & York

eprints@whiterose.ac.uk
https://eprints.whiterose.ac.uk/

Efficient acceleration of neutral atoms in laser produced plasmas

Malay Dalui[1,2]**, T. Madhu Trivikram**[1]**, James Colgan**[3]**, John Pasley**[4]**, and M. Krishnamurthy**[1,5,*]

[1]Tata Institute of Fundamental Research, 1 Homi Bhabha Road, Colaba, Mumbai 400 005, India
[2]Department of Physics, Lund University, P.O. Box 118, 221 00 Lund, Sweden
[3]Los Alamos National Laboratory, Los Alamos NM, 87545, USA
[4]York Plasma Institute, University of York, Heslington, York YO10 5DQ, UK
[5]TIFR Centre for Interdisciplinary Sciences, 21 Brundavan Colony, Narsingi, Hyderabad 500 075, India
[*]mkrism@tifr.res.in

ABSTRACT

Recent advances in high-intensity laser-produced plasmas have demonstrated their potential as compact charge particle accelerators. Unlike conventional accelerators, transient quasi-static charge separation acceleration fields in laser produced plasmas are highly localized and orders of magnitude larger. Manipulating these ion accelerators, to covert the fast ions to neutral atoms with little change in momentum, transform these to a bright source of MeV atoms. The emittance of the neutral atom beam would be similar to that expected for an ion beam. Since intense laser-produced plasmas have been demonstrated to produce high-brightness-low-emittance beams, it is possible to envisage generation of high-flux, low-emittance, high energy neutral atom beams in length scale of less than a milimeter. Here, we show a scheme where more than 80% of the fast ions are reduced to energetic neutral atoms and demonstrate the feasibility of a high energy neutral atom accelerator that could significantly impact applications in neutral atom lithography and diagnostics.

Introduction

Generating and analysing a beam of high energy neutral atoms is a challenge that is important for many technological applications[1–3]. In lithographic applications, high energy neutral atoms result in higher finesse structures than those produced with charged particle beams[4]. High energy hydrogen atom beams play an important role in Tokamak diagnostics[5]. The methods used to accelerate neutral atom have seen very little progress until quite recently[6–8].

The conventional techniques involve an ion source, accelerating columns and an efficient neutralizer, which employs either electron detachment (in case of negative ions) or electron capture (in case of positive ions) in a collision cell to convert ions to neutral atoms[9,10]. Charge changing atomic collisions lead to beam straggling and beam divergence that reduce the beam current delivered to the target[11]. Decreasing areal density (product of gas density and collision cell length) and a more efficient neutralization process can lead to a better emittance of the neutral atom beam.

The charge of a positively charged projectile can be reduced either by capturing a bound electron from a target atom (in a collision cell) or by capturing a free electron[12]. The capture cross-section increases as the binding energy of the electrons that are captured from the target atom becomes smaller[13]. If the velocity of the projectile is close to the orbital velocity of the bound electron in the target atom, the electron capture cross-section increases. There are three dominant routes for free electron capture by an atomic ion[12] : (a) radiative recombination, (b) dielectronic recombination and (c) three body recombination. In radiative recombination, the free electron capture is accompanied by radiation emission. The cross-section for this process is very low. Even for very highly charged ions (for instance, Ar^{18+}) and sufficiently low electron temperature ($\simeq 10$ eV), the cross-section is about $10^{-29} cm^2$[13]. Moreover, with increasing electron energy, the cross-section decreases dramatically. For Ar^{18+}, the cross-section is expected to decrease by about five orders of magnitude when the electron temperature increases from 5 eV to 10 eV[22]. Dielectronic recombination is the process by which the capture of a free electron leads to excitation of a bound electron in the host ion. The charge reduction is a two-step process whereby the de-excitation of the excited host ion in the second step leads to a charge-reduced system. Auto-ionization can deter the charge reduction. Since strong electrostatic fields are generated in high density plasmas, enhanced auto-ionization reduces the recombination rates. Three body recombination occurs when the electron density is high such that two electrons simultaneously interact with the atomic ion and one of the electrons is captured while the other (scattered) electron carries away the excess momentum.

In intense laser produced plasmas, it is possible to efficiently generate a burst of low energy electrons of high brightness.
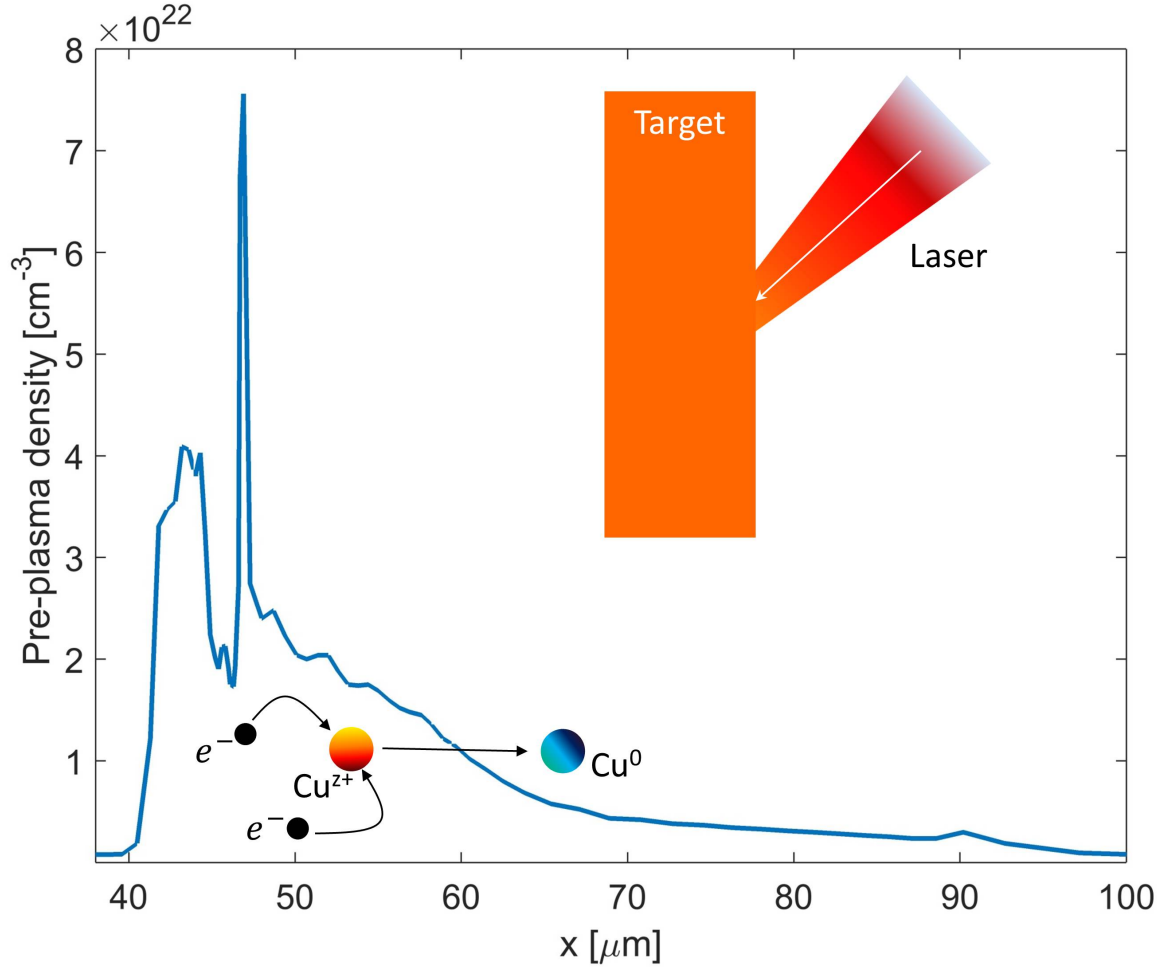
Figure 1. Neutral atom acceleration scheme: Intense laser-solid interaction produces strong transient fields and accelerates ions from the target surface. The pulse pedestal generates a pre-plasma (the electron density is shown here) and ions traversing through the pre-plasma undergo electron recombinations, dominated by three-body recombination, to become neutral atoms with little change in momentum. This paves the scheme for generating high energy neutral atom beams in intense laser produced plasmas.

Since electrons move faster than ions, they expand beyond the region of laser focus and can alter the recombination and charge transfer dynamics. Recently this was exploited to accelerate neutral atoms upto MeV energies[8]. Nano-clusters exposed to intense laser pulses leads to a very strong ionization. The electrons exploding from the clusters excite a large fraction of clusters beyond the focal volume to their Rydberg states. Coulomb exploded ions that traverse the Rydberg excited atomic clusters, where the charge transfer rates are orders of magnitude higher, undergo efficient neutralization. In just a few millimeters away from the laser focus almost 95% of the ions were observed to become neutral. While this proved the use of laser plasmas for enhanced charge transfer, there are two problems with this scheme that need attention for improving the generation of neutral beams. (a) Ion acceleration is achieved by Coulomb explosion of nano-clusters and the ion yields (consequently neutral atom yields) are orders of magnitude smaller than ion emission obtained from solid targets. (b) Ion emission is nearly isotropic and consequently the neutral-atom generation is also nearly isotropic. Ion acceleration from solid targets seems therefore to offer a more promising platform for energetic neutral atom generation. The interaction of high-intensity ultrashort laser-pulses accelerates ions along the target-normal direction by the target-normal-sheath-acceleration (TNSA) mechanism[14–18]. A high energy neutral atom source with the same emittance characteristics seen in ions generating from intense laser-produced plasma[19,20] would seem out of reach of conventional charge transfer methods of neutral atom generation. Charge transfer neutralization of ions accelerated in TNSA by using a gaseous medium is a possibility that has been demonstrated recently[21]. Instead of using a charge transfer cell for neutralization, if the TNSA accelerated ions could be neutralised in the laser produced
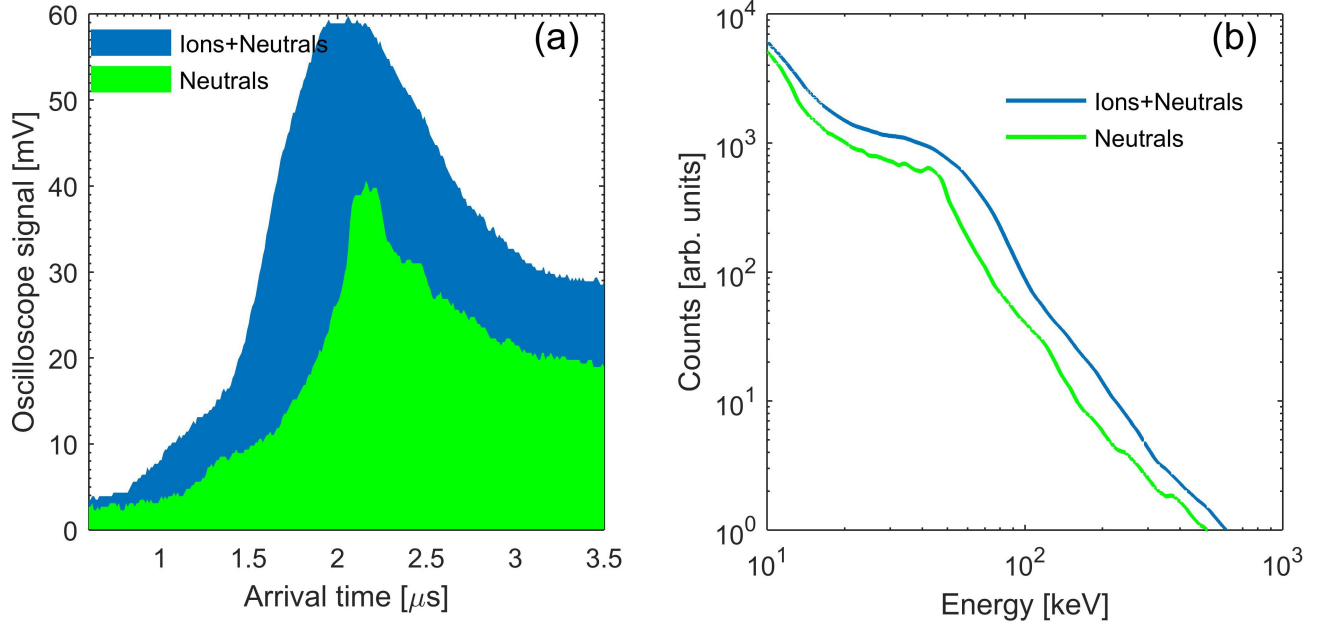
Figure 2. Arrival time profile and kinetic energy spectra. (a) shows the arrival time spectra of Cu atoms (TP is operated with high deflection fields to push ions out of the detector; green trace) and Cu ions (no deflection fields; blue trace). (b) shows the kinetic energy spectra of all Cu (ions and neutrals) and only the Cu neutrals as derived from the arrival times. The measurements are taken at a defocused position ($w \approx 50\ \mu$m).

plasma itself, then the generation of a beam of energetic neutral atoms with very high current could be achieved. The present work shows a successful scheme that achieves better neutralization using recombinations in plasma. High intensity laser produced plasmas are known to generate plasma with a high electron number density, it is conceivable therefore that the three body recombination may be exploited to convert the laser accelerated ions to neutral atoms.

The temporal profile of any intense femtosecond laser pulse does not normally resemble a delta function. Instead, in most laser systems (including ours), the pulse possess pedestal of much longer time duration before and after the ultrashort femtosecond part. This pedestal, though the intensity is one part of a million (of the peak), is large enough to produce plasma from a solid surface by multi-photon ionization[23]. This pre-plasma can be exploited as the neutralizer. Thus, our neutral atom accelerator involves two steps as illustrated in figure 1. First, the positive ions from a solid substrate are accelerated in the transient plasma fields created by the peak of the pulse. Second, the ions capture the free electrons in the plasma density that they traverse and are neutralized. Here, we demonstrate that under optimal conditions three body recombination can be dominant to achieve more than 80% ion-to-neutral conversion efficiency. We show an acceleration of the order of $10^{18}g$ (g is the acceleration due to gravity) in a length scale of a few hundred micrometers using a high-intensity laser-solid interaction.

Results and Discussion

The experiment was performed at the Tata Institute of Fundamental Research, Mumbai, India, using the high intensity short pulse laser facility. A Thomson parabola (TP)[24] and arrival-time (AT) measurement techniques were simultaneously employed to detect and characterize the accelerated neutral atoms[8] (see Methods for details). Figure 2 shows one of the measurement. Figure 2a and 2b shows the arrival time spectra of the detected particles (with and without the highest deflection field) and the derived kinetic energy spectra assuming all the atomic species to be Cu. This assumption is validated by independent charge-to-mass ratio resolved TP measurements that show that approximately 85% of the emitted ionic species are of Cu and hence the contribution of ions (C, O, H) originating from surface contamination, which are always present in laser-plasma experiments, are neglected. We have recorded on an average $\sim 10^{11}$ accelerated neutral Cu atoms per laser pulse. The ion divergence was measured and we infer that the half-angle at half-maxima of the transverse spatial extent of the neutrals (which would be same as in ions) is about 15-20° at the source. The maximum acceleration with 150 mJ laser pulse is found to be approximately a MeV.

In our quest of optimal conditions for neutralization, we find that the most effective method is to move the target towards the focusing parabolic mirror and defocus the laser focal spot. The laser spot size on the target (w) increases with increasing
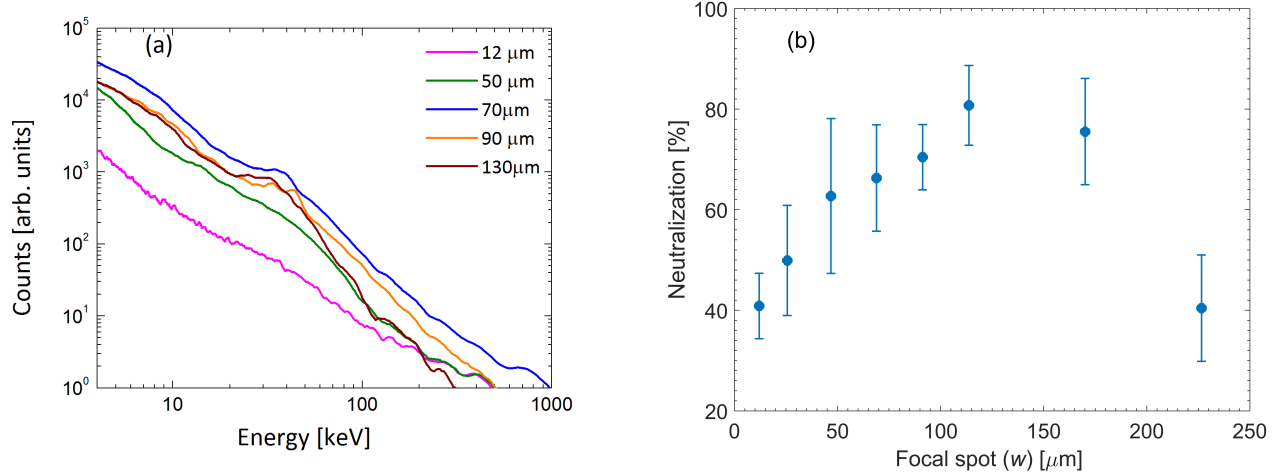
Figure 3. **Characterization of accelerated neutral atoms.** (a) shows the kinetic energy spectra of the neutral Cu-atoms, and (b) the neutralization fraction as derived from the AT signal at different defocused spot (w).

defocusing. Figure 3a shows the energy spectra of the neutral atoms with laser defocusing as derived from the AT signals when 150 mJ pulses (the corresponding intensity when $w \approx 12$ μm is $\approx 10^{18}$ W/cm^2) are incident on the target. The ion acceleration appears to increase with the focal spot and the smallest spot size is not necessarily optimal for highest acceleration. The total neutralization fraction (energy integrated) as a function of the laser focal waist size is shown in figure 3b. Increasing the focal spot size not only decreases the laser intensity, but also lowers the intensity of the pulse pedestal responsible for pre-plasma generation. A lower intensity pre-plasma decreases the electron density but more importantly it decreases the pre-plasma electron temperature[25]. The cold electron temperature is expected to scale linearly with the laser intensity[26]. Therefore, a ten fold increase in spot size will bring in a 100 fold decrease in both focused laser intensity and electron temperature. The cold electron temperature of the plasma (at $w \approx 12$ μm) in our experiments is about 300 eV[27] and so, in the defocused condition, the pre-plasma temperature is expected to be about a few eV or less. Beyond the optimal defocusing the pre-pulse level goes below the pre-plasma formation threshold. The main pulse intensity also becomes low for effective ion acceleration. Hence, both the ion acceleration and the neutralization are diminished. Defocusing thus brings about two crucial changes: (a) the electron temperature of the pre-plasma is lowered dramatically with much smaller changes in electron density, and (b) the average charge states of the accelerated (by the main pulse) Cu ions are expected to be lower as the laser pulse intensity is decreased. Lowering the average charge states makes the neutralization easier since, on average, fewer electron transfer steps are needed.

The experiments were carried out in a vacuum chamber maintained at $\approx 10^{-5}$ mbar. Since mean free path is more than 10 meters (compared to ion traversal length of about a meter), charge transfer collisions of the ions with the background gas can be neglected. Their contribution to the neutralization is computed to be less than 1%. To understand the neutralization process, we first need information of the pre-plasma profile in which the ion traverse before reaching the detector. We use the HYADES one dimensional radiation hydrodynamics simulation code to obtain the electron density and temperature profiles of the pre-plasma as a function of the distance away from the target front surface (set at $x = 0$). The simulations take the measured laser pre-pulse and employ a lagrangian radiation hydrodynamics solver incorporating multi-group radiation diffusion and a flux limited diffusion model for electron-thermal conduction. Figure 4 gives the results for two different defocusing conditions used in the experiments labelled by the focal waist (w). The computations show peaks in electron density due to the formation of shock waves driven by the laser pre-pulse leading to a rarefaction wave into the target.

As ions traverse this plasma profile, neutralisaion occurs and to fully capture the charge reduction dynamics, we have used the ATOMIC code developed at the Los Alamos National Laboratory, USA. ATOMIC is a multi-purpose plasma kinetics code[28,29] that is used for modelling local thermodynamic equilibrium (LTE) and non-LTE plasmas, and can predict ionization balances, opacities and emissivities for a wide range of plasma conditions. The code takes as input atomic structure and collision data from the Los Alamos suite of atomic physics codes (for an overview, see[30]). In this case, the CATS code[31,32] was used in configuration-average mode to generate structure data and electron-impact excitation cross-sections for all ionization stages of Cu. The GIPPER code[30,33] was then used to generate all possible ionization cross-sections. ATOMIC was run in steady-state non-LTE mode[34] (assuming zero radiation temperature) and used the electron temperature, density values and the initial average charge of the ions starting from the surface of the solid target produced by HYADES as input, resulting in predictions of the average ionization and charge distribution at each set of plasma conditions. Convergence tests with respect to
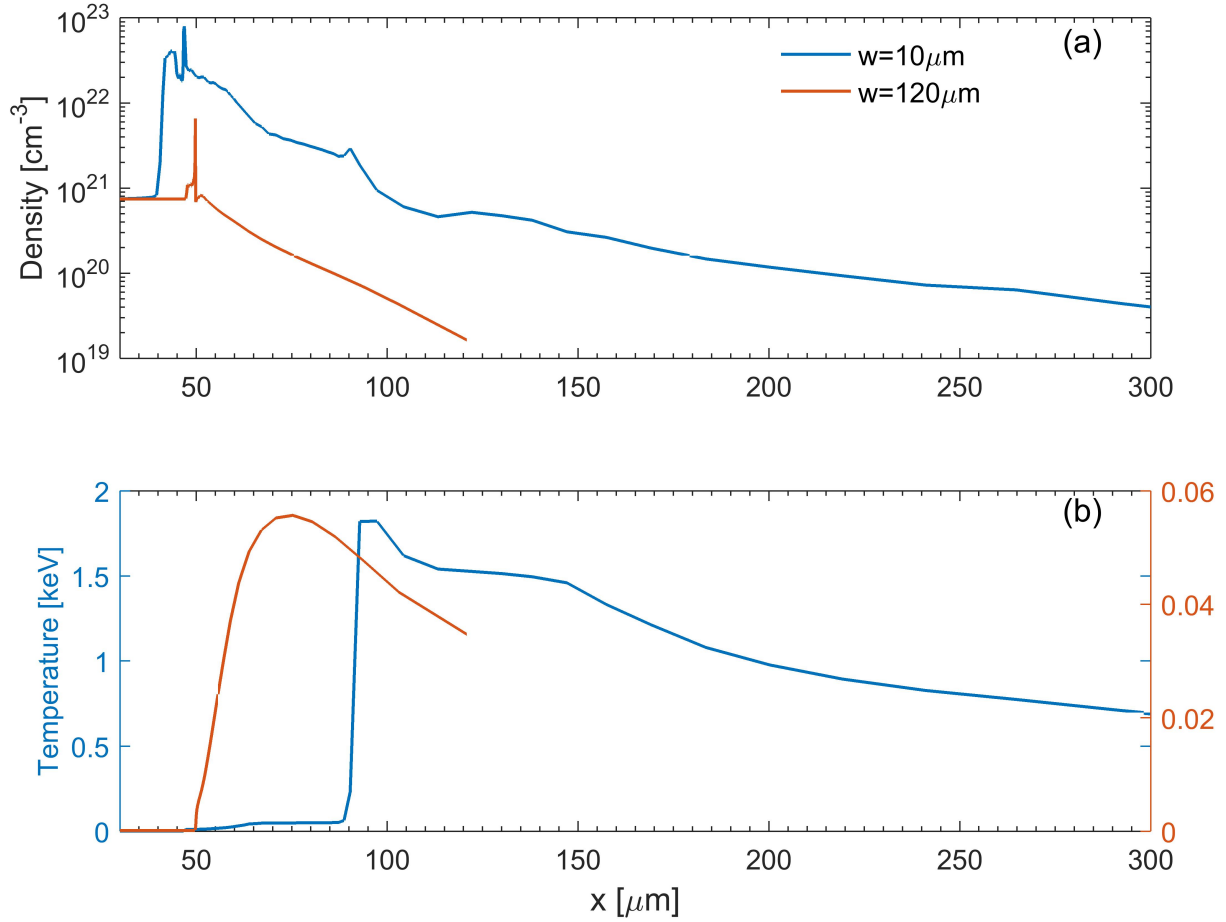
Figure 4. Pre-plasma profile. The electron density and temperature for two different focal waist conditions are generated using HYADES 1-D radiation hydrodynamics code using SESAME EOS and a multigroup radiation diffusion approximation. Data is presented at the end of the pre-pulse. The final intensity point is taken 1 picosecond prior to the arrival of the main pulse.

the number of configurations included for each ionization stage were performed to ensure that the resulting average ionization predictions are converged. Since propagation of the HYADES code to long distances was computationally prohibitive, the electron temperature and density from figure 4 were extrapolated using an exponential scaling.

In figure 5 we show the change in the average charge state ($\bar{Z}$) of Cu ions computed as a function of the distance traversed from the target surface for the focal waists of 10 μm and 120 μm. We find that, for both cases, the ions eventually recombine to form neutral atoms (corresponding to $\bar{Z} = 0$). At the larger focal waist ($w = 120$ μm) the ions start with a lower average charge and the overall recombination rates are larger, resulting in faster neutralization. In both of these cases, at any given distance the charge state is much lower with the larger focus than at the tight focus condition and so the neutralization fraction is expected to be larger with the larger focal waist. Although the ATOMIC codes includes all the possible recombination process, we find that three-body recombination plays a dominant role, but that dielectronic recombination is also quite important. We note that it is very difficult to fully compute the neutralization fraction found in the experiments due to many issues. For example, we will need to know more precisely the charge histogram at the front surface as the focal waist is changed. We also realize that apart from the pulse pedestal, the main pulse also changes the electron density and electron temperature profile. 2-D effects will play a role in the hydrodynamics and these will also affect the neutralization process. These results however demonstrates that tailoring the pre-plasma by means of defocusing is a viable option for increasing the neutralization fraction. The pre-plasma electron temperature plays a crucial role in increasing the rate of three-body recombination and dielectronic recombination at larger focal waists.

In summary, a compact neutral atom acceleration technique yielding a beam of neutral atoms with more than 80%
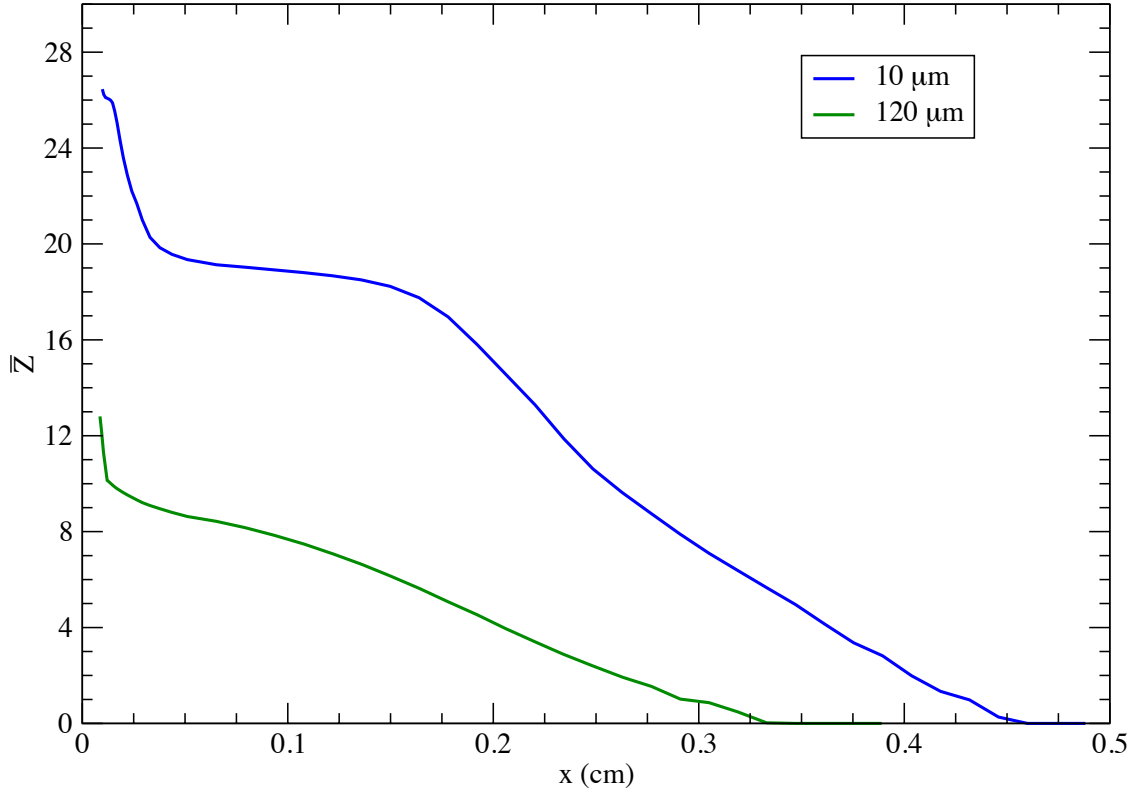
Figure 5. Evolution of the average charge state. Change in the average charge state ($\bar{Z}$) of the Cu ions as they propagates through the pre-plasma, away from the target surface. The pre-plasma density and temperatures computed by the HYADES code (see figure 4) are used to compute the electron recombination rates using ATOMIC code.

neutralization efficiency from a laser-produced plasma has been experimentally realized. Acceleration up to an MeV energy has been achieved by this scheme (the corresponding acceleration is $\sim 10^{18}g$). The neutral atom yield as well as the ion-to-neutral conversion efficiency has been seen to increase with laser defocusing. The neutral atom acceleration process involves two steps. First, ions formed at the target surface are accelerated in the sheath electric field and second, electron recombination, dominated by three body recombination, results in charge reduction and neutralization without any significant change in momentum. The emittance of the neutral atom remains the same as the ions and the neutral atoms emanate from a spot of approximately 100 μm diameter, expanding normal to the target in a $15°$ cone.

Methods

In the experiment 800 nm, 40 fs, p-polarized laser pulses were used from a CPA-based[35] Ti:sapphire laser system, capable of delivering light pulses at a repetition rate of 10 Hz. The laser pulse was focused on the target using a couple of guiding mirror and an off-axis parabolic mirror at an incidence angle of about $40°$. A 5 cm×5 cm×5 mm Cu substrate was used as the target. The front surface of the target, where the laser pulse was incident, is optically flat. It was placed on a x-y-z-θ stage assembly to enable for raster scanning such that every time the incident laser pulse sees a undamaged part on the Cu-substrate. Defocusing was done by moving the target towards the target normal direction (z-direction). The generated particles were diagnosed using a Thomson parabola spectrometer, coupled with a micro-channel-plate (MCP) detector and a CCD camera, placed at a meter away from the target. As in any typical Thomson spectrometer, electric and magnetic fields were applied

in parallel direction to disperse ions into parabolic traces according to their charge-to-mass ratio. Simultaneous imaging and arrival time measurements were used to detect and measure the energy of the accelerated neutral atoms. If the field (either the electric or the magnetic field) in the TP is small, ions would be dispersed in a straight line. The field was then increased until all the ions were deflected out of the detector. At this configuration, the TP-spectrogram was left only with the central bright spot. Neutral atoms and the photons unaffected by any electric field and/or magnetic field, were detected in this central spot. We have used only the magnetic field to deflect the ions for neutral atom detection to avoid re-ionization of the neutrals in the field region of the spectrometer. After ensuring that the detector was exposed only to neutral particles, we measured the arrival time of the particles. Photons travel at the speed of light and reach the detector within a few nanoseconds, whereas the more massive neutral atoms arrive at the detector at microsecond time scales. From the arrival time profile the energy spectra and the percentage of neutralization can be easily extracted.

References

1. Osher, J. E. *Plasma Diagnostic Techniques* (ed. Huddlestone R. H. & Leonard S. L.) (Academic Press, New York, 1965).

2. Hutchinson, I. H. *Principles of Plasma Diagnostics* (Cambridge University Press, New York, 1987).

3. Gruntman, M. Energetic neutral atom imaging of space plasmas. *Rev. Sci. Instrum.* **68**, 3617 (1997).

4. Wolfe, J. C. & Craver, B. P. Neutral particle lithography: a simple solution to charge-related artefacts in ion beam proximity printing. *J Phys.* D **41**, 024007 (2008).

5. Rej, D. J., Henins, I., Fonck, R.I. & Kim, Y.J., Intense diagnostic neutral beam development for ITER. *Rev. Sci. Instrum.* **63** 4934-4936 (1992).

6. Eichmann, U., Nubbemeyer, T., Rottke, H. & Sandner, W. Acceleration of neutral atoms in strong short-pulse laser fields. *Nature* **461**, 1261-1265 (2009).

7. Maher-McWilliams, C., Douglas, P. & Barker, P. F. Laser-driven acceleration of neutral particles. *Nat. Photonics* **6**, 386-390 (2012).

8. Rajeev, R. *et al.* A compact laser-driven plasma accelerator for mega electronvolt energy neutral atoms. *Nat. Phys.* **9**, 185-190 (2013).

9. Dimov, G. I. & Roslyakov, G. V. Conversion of a beam of negative hydrogen ions to atomic hydrogen in a plasma target at energies between 0.5 and 1 MeV. *Nucl. Fusion* **15**, 551 (1975).

10. Wells, N. *Production of Neutral Beams from Negative Ion Beam Systems in the USSR*, (Santa Monica, CA: RAND Corporation, 1982).

11. Giuntini, L. A review of external microbeams for ion beam analyses. *Anal Bioanal Chem* **401**, 785-793 (2011).

12. McDaniel, E. W., Mitchell, J. B. A. & Eugene Rudd, M. *Atomic Collisions: Heavy Particle Projectiles* (Wiley, 1993).

13. http://open.adas.co.uk/

14. Clark, E. L. *et al.* Measurements of Energetic Proton Transport through Magnetized Plasma from Intense Laser Interactions with Solids. *Phys. Rev. Lett.* **84**, 670 (2000).

15. Maksimchuk, A., Gu, S., Flippo, K., Umstadter, D. and Bychenkov, V. Yu. Forward ion acceleration in thin films driven by a high-intensity laser. *Phys. Rev. Lett.* **84**, 4108 (2000).

16. Snavely, R. A. *et al.* Intense high-energy proton beams from petawatt-laser irradiation of solids. *Phys. Rev. Lett.* **85**, 2945 (2000).

17. Hatchett, S. P. *et al.* Electron, photon, and ion beams from the relativistic interaction of Petawatt laser pulses with solid targets. *Phys. Plasmas* **7**, 2076 (2000).

18. Wilks, S. C. *et al.* Energetic proton generation in ultra-intense laser-solid interactions. *Phys. Plasmas* **8**, 542-549 (2001).

19. Rosenzwig J. & Serafini L. *The physics of high brightness beams* (World Scientific publishing, 2000).

20. Cowan, T. E. *et al.* Ultralow Emittance, Multi-MeV Proton Beams from a Laser Virtual-Cathode Plasma Accelerator. *Phys. Rev. Lett.* **92**, 204801 (2004).

21. Mollica F. *et al.* Efficient laser production of energetic neutral beams, *Plas. Phys. Control Fusion* **58**, 034016 (2016).

22. Rajeev R., Ph.D Thesis (2012).

23. Gibbon, P. *Short Pulse Laser Interactions with Matter, an introduction*, (Imperial College Press, London, UK, 2005).

24. Dalui, M., Madhu Trivikram, T., Ram Gopal & Krishnamurthy, M. Probing strong field ionization of solids with a Thomson parabola spectrometer. *Pramana-J. Phys.* **82**, 111 (2014).

25. Xu, M. H. *et al*. Enhancement of ion generation in femtosecond ultraintense laser-foil interactions by defocusing. *Appl. Phys. Lett.* **100**, 084101 (2012).

26. Kruer W. L. *Physics of Laser Plasma interaction*, (Westview press, 2003).

27. Mondal S. *et al.* Doppler Spectrometry for Ultrafast Temporal Mapping of Density Dynamics in Laser-Induced Plasmas. *Phys. Rev. Lett.* **105**, 105002 (2010).

28. Magee N. H. *et al.*, Los Alamos Opacities: Transition from LEDCOP to ATOMIC, 14th Topical Conference on Atomic Processes in Plasmas, (Eds: J.S. Cohen, S. Mazevet, D.P. Kilcrease, AIP Conference Proceedings, New York, 2004) 168-179.

29. Hakel P. *et al*. The new Los Alamos Opacity Code ATOMIC. *J. Quant. Spectr. Rad. Transfer* **99**, 265 (2006).

30. Fontes C. J. *et al.* The Los Alamos suite of relativistic atomic physics codes. *J. Phys. B* **48**, 144014 (2015).

31. Cowan R. D. *The Theory of Atomic Structure and Spectra*. (University of California Press, Berkeley, 1981).

32. Abdallah J., Clark, R. E. H. & Cowan R. D. CATS: Cowan atomic structure code, Los Alamos National Laboratory, Los Alamos Manual No. LA 11436-M-I (1988).

33. Clark R. E. H., Abdallah Jr, J. & Mann J. B. Integral and differential cross sections for electron impact ionization. *Ap. J.* **381**, 597-600 (1991).

34. Fontes C. J., Colgan J. & Abdallah, Jr., J. *Modern Methods in Collisional-Radiative Modeling of Plasmas* (Ed. Ralchenko, Y) (Springer, Switzerland, Editor: Yu. Ralchenko, 2016).

35. Strickland, D. & Mourou, G. Compression of amplified chirped optical pulses. *Opt. Commun* **56**, 219 (1985).

Acknowledgements

Author contributions

Experimental measurements were performed by M.D. and T.M.T. under the guidance of M.K. The data analysis were carried out by M.D. J.C. computed the electron recombination dynamics in the ATOMIC simulation and J.P. carried out the HYADES hydrodynamic simulations. All authors contributed to the drafting of the manuscript.

Competing financial interests

The authors declare no competing financial interests.